ABHD2 activity is not required for the non-genomic action of progesterone on human sperm

Oliver Arnolds[1*], Eve M. Carter[2*], Madison Edwards[3*], Edvard Wigren[1], Evert Homan[4], Pauline Ribera[5], Kirsty Bentley[4] Martin Haraldsson[5] Nmesoma Theo-Emegano[3], Peter Loppnau[3], Magdalena M Szewczyk[3], Michelle A Cao[3], Dalia Barsyte-Lovejoy[3], Karen Vester[6], Anna Thrun[6], Alexandra Amaral[6], Ralf Lesche[6], Jens Münchow[7,8], W. Felix Zhu[7,8], Louisa Temme[8,9], Christoph Brenker[10], Timo Strünker[8,10], Michael Sundström[1], Matthew H. Todd[2], Aled M Edwards[3], Claudia Tredup[11,12 ¶], Opher Gileadi[1, ¶]

1. *Structural Genomics Consortium (SGC) and Center for Molecular Medicine, Department of Medicine, Karolinska Institute, Stockholm, Sweden*
2. *School of Pharmacy and Structural Genomics Consortium, University College London, London, UK*
3. *Structural Genomics Consortium (SGC), University of Toronto, Toronto, Canada*
4. *Department of Oncology-Pathology, Karolinska Institutet, Stockholm, Sweden*
5. *Chemical Biology Consortium Sweden (CBCS), Science for Life Laboratory, Department of Medical Biochemistry and Biophysics, Karolinska Institutet, Stockholm, Sweden*
6. *Nuvisan ICB GMBH, Berlin, Germany*
7. *Institute of Pharmaceutical and Medicinal Chemistry, University of Münster, Germany*
8. *GRK 2515, Chemical Biology of Ion Channels (Chembion), University of Münster, Germany*
9. *Institute of Pharmacy, University of Hamburg, Hamburg,Germany*
10. *Center of Reproductive Medicine and Andrology, University of Münster, University Hospital Münster, Germany*
11. *Institute of Pharmaceutical Chemistry, Goethe University Frankfurt, Frankfurt, Germany.*
12. *Structural Genomics Consortium, BMLS, Goethe University Frankfurt, Frankfurt, Germany*

¶ Corresponding authors. tredup@pharmchem.uni-frankfurt.de , opher.gileadi@ki.se

** equal contribution*

Abstract

Sperm activation is controlled by an influx of calcium ions through the CatSper channel, which is activated in the oviduct by a non-genomic action of progesterone. Progesterone has been hypothesized to act as an activator of ABHD2 activity, which in turn hydrolyses 1- and 2-arachadinoyl glycerol, putative inhibitors of CatSper. To explore the idea of targeting ABHD2 activity as a contraceptive target, we synthesized derivatives of published ABHD2 inhibitors, optimizing for potency and in-cell target engagement, and tested active inhibitors and structurally-related inactive derivatives in sperm motility assays and calcium influx assays. We observed no effect of ABHD2 inhibition on basal or progesterone-induced activity in both assays. We also found no evidence for direct binding of progesterone to purified recombinant

ABHD2 protein. We conclude that ABHD2 activity is not required for the non-genomic action of progesterone on human sperm.

Introduction

It is estimated that 164 million women still have an unmet need for family planning[1]. While hormonal contraceptives are widely used and highly effective, increasing numbers of women are reluctant to use them due to side effects and safety concerns[2]. Despite this, the options for reversible, non-hormonal contraceptives with high efficacy remain very limited[3]. Only copper intrauterine devices (IUDs) reach efficacies higher than 99 %, but their use is also frequently discontinued due to side effects[4–8]. Innovative approaches for non-hormonal contraception aim to inhibit key protein targets by small molecule inhibitors at various levels of intersection, e.g., spermatogenesis, oogenesis, sperm function, or fertilization.[3] Such an approach requires identification and comprehensive characterization of the potential target proteins.

Elevation of intracellular Ca^{2+} levels is a fundamental signaling element of spermatozoa maturation, motility, as well as the acrosome reaction, and is therefore crucial for fertility[9,10]. The increase in intracellular Ca^{2+} levels in human sperm is mediated by the sperm-specific cation channel CatSper, which is activated by an alkaline pH in the oviduct and a non-genomic response to progesterone secretion by cumulus cells that surround the oocyte[11–13]. It has been proposed that CatSper activation can be inhibited by the irreversible metabolic serine-hydrolase-inhibitor methyl arachidonoyl fluorophosphate (MAFP) or endocannabinoids 1- and 2-arachadinoyl glycerol (1- and 2-AG), the latter of which are thought to be enriched in membranes of spermatozoa and depleted after stimulation with progesterone[14]. The subsequent influx of Ca^{2+} leads to hyperactivation. This change in the motility pattern enables the capacitated spermatozoon to navigate from the oviductal reservoirs through viscoelastic luminal fluids, as well as the cumulus oophorus, finally allowing them to penetrate the zona pellucida, a glycoprotein-rich layer surrounding the oocyte[15–19]. This triggers the acrosome reaction, leading to the fusion of the sperm and oocyte[20–22]. Regulation of CatSper activation has therefore been regarded as a promising strategy for the development of new contraceptives.

The α/β hydrolase domain 2 (ABHD2) has been proposed as the non-genomic progesterone receptor responsible for CatSper activation in spermatozoa[14]. ABHD2 is a member of a family of serine hydrolases, and was described as an extracellular domain anchored to the flagellum membrane of spermatozoa[14,23]. Due to modulation of CatSper in the presence of endogenous steroids, e.g., progesterone, testosterone, or hydrocortisone, it was suggested that these steroids regulate enzymatic activity of ABHD2[13,14,24–26]. Further, decreased mRNA levels for ABHD2 and frame-shift mutations were detected in infertile men displaying

oligoasthenospermia, which is clinically characterized by decreased number of sperm as well as decreased sperm motility[27,28]. One paper reports an elevation of ABHD2 mRNA in spermatozoa stimulated by progesterone, alongside increases of cAMP and PKA activity, suggesting that ABHD2 is involved in cAMP signaling in spermatozoa[27].

Based on these findings, ABHD2 was proposed to be a promising target for contraceptives[24,29]. However, the absence of suitable reagents has hindered a comprehensive investigation of this enzyme as a contraception target and the associated molecular mechanisms. Here, we describe (1) the development of potent and selective inhibitors of ABHD2, (2) their use in probing the effects of ABHD2 inhibition on the function of sperm cells and (3) the implications for the use of ABHD2 activity as a target for contraception.

Results

Production and enzymatic activity of recombinant ABHD2

We have expressed and purified the full-length (FL) human ABHD2 protein in baculovirus-infected insect cells and used this protein to identify appropriate substrates for enzymatic assays and characterize initial inhibitors. To develop enzymatic screening assays, we tested fluorogenic substrates that were previously used for lipid hydrolases: resorufin butyrate (RB), 4-methylcoumarin butyrate (4MC-B), and 7-hydroxycoumarinyl arachidonate (7-HCA)[30–33]. The purified full-length ABHD2 showed enzymatic activity towards the three substrates (4MC-B: K_m = 27 µM. 7-HCA: K_m = 60 µM. RB: K_m = 22 µM. Supplementary figure S1). 7-HCA was chosen as the substrate for subsequent assays, because of its high signal to background ratio. We note that the RB substrate can be used as an alternative in conjunction with compounds that interfere with the fluorescence detection of 7-HCA.

We then assessed the potency of several tool compounds towards FL-ABHD2 (Figure 1A and Supplementary Figure S1A). In line with our expectations, MAFP inhibited ABHD2 with an apparent IC_{50} of 40-50 nM. Orlistat inhibited FL-ABHD2 with sub-µM IC_{50}s (IC_{50} = 230 nM). Compounds **1** and **3** inhibited FL-ABHD2 with apparent IC_{50}s of ~100 nM. Pristimerin and lupeol, which were proposed to inhibit ABHD2[2], did not inhibit FL-ABHD2 in the concentration range tested.

We also designed multiple constructs for expression in *E. coli*. Our attempts to express and purify the full-length ABHD2 protein were unsuccessful, but replacement of the first 32 amino acids with a His-Flag tag resulted in expression of a stable protein in *E. coli* cells. The deleted N-terminus is predicted by Alphafold2 to form a hydrophobic alpha helix that protrudes from

the globular structure of the central portion of the protein[34]. possibly forming a transmembrane anchor tethering ABHD2 to the membrane. Unless indicated otherwise, ABHD2 protein used in subsequent assays was the truncated version (L33-E425).

Bacterially-expressed ABHD2 (L33-E425) purified on size exclusion chromatography as a tetramer (confirmed by mass photometry; data not shown). Its enzymatic activity was assayed using 7-HCA, which exhibited K_m and k_{cat} of 280 nM and 2.8 pmol substrate/min/pmol enzyme, respectively (Supplementary figure S2). The reason for the discrepancy of this K_m value from the value reported for full-length ABHD2 is unclear. ABHD2's hydrolase activity was also inhibited by MAFP (methoxy arachidonyl fluorophosphonate), a non-specific covalent hydrolase inhibitor.

Urea-based compounds inhibit ABHD2 activity

Baggelaar et al. used activity-based protein profiling to identify the urea-based compound 1 (compound 183 in the original paper) as an inhibitor of ABHD2[29]. The compound demonstrated protection of the active site from covalent modification in cell lysates as well as reduced acrosome reaction of murine spermatozoa[29]. We tested compound 1 with purified ABHD2 (L33-E425) and full-length ABHD2 and observed inhibition of enzymatic activity as well as thermal stabilization (Figure 1 and Supplementary figure 1). Compound 3, a reported inhibitor of diacylglycerol lipase β (DAGLβ) as well as ABHD6[35,36], also potently inhibited both the full-length and (L33-E425) ABHD2 enzymes.

Based on these results, we purchased and synthesized 69 compounds that were tested for inhibition of ABHD2 at a concentration of 10 µM. Of those, three compounds (**2**, **4** and **5**) with sub-micromolar IC50 values were selected. In addition, two similar but inactive compounds (**6** and **7**) were used as negative controls (Figure 1). Compounds **2, 3, 4** and **5** led to stabilization of the enzyme as measured by Differential Scanning Fluorimetry (DSF) of between 3 and 14°C; in contrast, the negative control compounds **6** and **7** led to much lower stabilization, if any. Notably, these compounds did not inhibit the enzymatic activity of ABHD10 and ABHD11 (see Supplementary figure 3). Compounds **1** and **2**, initially tested as racemic mixtures, were separated into the enantiomers which were then assayed separately. For both compounds, the *(R)*-enantiomer displayed higher potency, with a greater difference seen for compound 2, (Figure 1 and Supplementary figure 4), supporting a binding event with the chiral protein.

The triazole urea compound 3 inhibits certain serine hydrolases by covalent modification of the catalytic serine residue[35,36]. Covalent modification of ABHD2 (L33-E425) by compound **3** was confirmed via mass spectrometry, but was not observed for compounds **1**, **2**, **4** or **5** (Supplementary Figure S5). Furthermore, no covalent modification by compound **3** was

observed for an inactive mutant of ABHD2, in which the catalytic serine was mutated to an alanine (S207A; Supplementary figure 6).

ABHD2 activity is not affected by steroids

A key aspect of the proposed role of ABHD2 in sperm activation is its activation by progesterone[13,14,24]. Other steroids such as testosterone, hydrocortisone, estrogen and the plant triterpenoids lupeol and pristimerin were suggested as modulators of ABHD2 activity and thereby of CatSper activation in human spermatozoa[24,26,37]. These steroids and the plant triterpenoids were proposed to antagonize the activation of CatSper by progesterone. However, subsequent studies indicated that testosterone, hydrocortisone, and estradiol are, in fact, also true CatSper agonists and that lupeol and pristimerin do not antagonize CatSper activation by progesterone.[26,37] Cholesterol was also discussed as a potential inhibitor of progesterone-mediated sperm function by potentially inhibiting ABHD2 activity[25]. As a direct interaction between ABHD2 and endogenous steroids has not yet been demonstrated, we tested for binding and influence of several steroids on the enzymatic activity of ABHD2 (L33-E425). We did not observe a substantial effect on enzymatic activity, neither activation nor inhibition, for any of the tested substances at 10 µM. This concentration exceeds the reported sub-micromolar inhibitory or effective concentrations for testosterone, 17β-estradiol, hydrocortisone, progesterone, and 17α-hydroxyprogesterone that were reported to influence Ca^{2+} influx in sperm by factors of 12 to 314. (Figure 2A)[24,38]. Only pristimerin led to complete inhibition of enzymatic activity (Figure 2A), although it did not inhibit full-length ABHD2 (Supplementary figure 1C).

We also assessed the binding of steroids to ABHD2 by DSF. No thermal stabilization of ABHD2 was observed after 30 minutes of pre-incubation with progesterone, cholesterol, testosterone, pregnenolone sulfate, hydrocortisone, or 17 α-hydroxyprogesterone at 40 µM (Figure 2B). Determination of melting temperatures for 17β-estradiol and pristimerin was unsuccessful, as the molecules interfered with the fluorescence signal. In agreement with the results of the truncated protein, the activity of full-length ABHD2 was unaffected by progesterone. Full-length ABHD2 also showed no thermal stabilization upon addition of progesterone compared to the DMSO control (Supplementary figure 7). As a positive control we used compound **1**, which showed a thermal stabilization of the full-length ABHD2 protein by 6.5°C.

Target engagement of cellular ABHD2 by small molecule inhibitors.

It has been suggested that the catalytic domain of ABHD2 is extracellular, located on the surface of sperm cells[14,23]. We sought to clarify this point by expressing a full-length ABHD2

protein with a C-terminal flag tag in transfected U2OS cells, which were then either permeabilized or not before incubation with mouse anti-flag antibodies. In permeabilized cells fluorescence signal was detected in the outside of the nucleus throughout the cell. Non-permeabilized cells displayed weaker fluorescence signal, also mainly from the cytoplasm (Supplementary figure 8). This suggests that ABHD2 is not localized predominantly at the extracellular plasma membrane in transfected U2OS cells. We tested, therefore, whether the inhibitors could engage ABHD2 inside cells.

We assessed target engagement in cells by monitoring thermal denaturation of ABHD2 in whole cells. HEK293T cells were transfected with ABHD2 (L33-E425) carrying an N-terminal HiBit tag. Cells were incubated with 5 µM of compound **1**, the negative control compound **6** or DMSO followed by an incubation for 3 minutes at temperatures ranging from 37°C to 60°C. Compound **1** stabilized intracellular ABHD2 by 1.9°C compared to DMSO or the negative control (Figure 3A). For examining multiple compounds, a single heating temperature of 50°C was selected, and compared with cells incubated at 37°C. This was performed with *(R)*-**1**, *(S)*-**1**, **2**, *(R)*-**2**, *(S)*-**2**, **3, 4**, **5**, the negative controls **6** and **7**, or DMSO. Recovery of signal of 20-50 % was observed for all identified hit compounds, compared with 10% for DMSO or the negative controls (Figure 3B). The highest stabilization was observed with the most potent compounds **2**, *(R)*-**2**, and **5**. This indicates that these compounds penetrate the cell membrane and engage the target protein ABHD2. The single exception was compound **3**, which precipitated at the tested concentration.

Inhibition of ABHD2 does not prevent sperm hyperactivation

To test the hypothesis that ABHD2 mediates the effect of progesterone (P4) in inducing human sperm hyperactivation, human sperm samples were incubated for 1 h with 10 µM of a) compound **1**; b) compound **3**; c) MAFP; d) lupeol and e) pristimerin; before adding P4. Two controls were included: a) DMSO (used to dissolve P4 and the inhibitors); b) P4 without any inhibitor.

As expected, P4 induced a statistically significant increase in the fraction of hyperactive sperm (Figure 4). Pre-incubation with the ABHD2 inhibitor compounds **1, 3**, MAFP and lupeol, did not inhibit the action of P4 (no differences were found between these and P4 alone; and all were statistically different from DMSO control). Pristimerin completely inhibited sperm motility in all samples tested, and as such hyperactivation could not be assessed. Altogether, the outcomes suggest that ABHD2 has no impact on human sperm hyperactivation.

Finally, we studied the action of the ABHD2 inhibitors **3** and *(R)*-**2**, the ABHD2-inactive compound **6**, and the CatSper inhibitor TS150[39] on the intracellular Ca^{2+} concentration $[Ca^{2+}]_i$

and progesterone-induced Ca^{2+} signals in human sperm; $[Ca^{2+}]_i$ was monitored using the fluorescent Ca^{2+} indicator Fluo4. The ABHD2 inhibitor and the ABHD2-inactive compound evoked miniscule changes in $[Ca^{2+}]_i$, but did not affect the progesterone-induced Ca^{2+} signal (Figure 5A-E). By contrast, the CatSper inhibitor TS150 completely abolished the progesterone response (Figure 5A-E). These results align with that of the motility experiment, demonstrating that ABHD2 activity is not required for progesterone-evoked Ca^{2+} signals and motility responses in human sperm.

Discussion

The mechanism underlying the activation of the CatSper channel and the subsequent Ca^{2+} flux in human spermatozoa is not fully understood. Progesterone-, pregnenolone sulfate-, and 17α-hydroxyprogesterone-induced activation of the channel has been reported[13,24,26], and other steroids such as testosterone, hydrocortisone, 17β-estradiol, and cholesterol have been suggested to be either agonists or antagonists[24–26,37]. Contrary to the proposed role of ABHD2 as a non-genomic steroid receptor[14,24,25,23], we observed that ABHD2 (L33-E425) enzymatic activity is unaffected by progesterone, pregnenolone sulfate, testosterone, hydrocortisone, or cholesterol. None of the steroids tested provided thermostabilization of ABHD2, in contrast with small-molecule inhibitors. Progesterone also did not affect the enzymatic activity nor the thermostability of full-length, purified ABHD2. There are also conflicting results concerning the effect of pristimerin and lupeol on CatSper activation [24,26, 34]. While our data does not provide more information on the direct effects of lupeol or pristimerin on CatSper, lupeol did not affect the enzymatic activity nor the thermostability of purified ABHD2. Our data demonstrate that ABHD2 enzymatic activity is not affected by steroids, as they neither inhibited nor stimulated enzymatic activity *in vitro*. This indicates that the activation of CatSper by steroids follows a different mechanism which does not involve ABHD2 activity.

ABHD2's role in hyperactivation of human spermatozoa was proposed based on the enzymatic activity of serine hydrolases. These enzymes reportedly deplete 2-AG upon progesterone activation, resulting in Ca^{2+}-influx. This influx was be blocked by pre-incubation with the irreversible serine hydrolase inhibitor MAFP[14]. Here, we developed three more potent ABHD2 inhibitors, based on a specific inhibitor previously identified by Baggelaar et al.[29] We also demonstrate inhibition and covalent modification of ABHD2 by compound 3, previously identified as a selective inhibitor of ABHD6 and DAGLβ. Using thermostabilization assays in intact transfected HEK cells, we demonstrate that compounds **1, *(R)*-1, *(S)*-1, 2, *(R)*-2, *(S)*-2,**

4 and **5** engage ABHD2. These compounds, along with the negative control compound, provide a powerful tool kit to test hypotheses around the biological activity of ABHD2.

We then used the tool compounds to examine the role of ABHD2 in progesterone-dependent human sperm activation. Pre-incubation of human sperm with these compounds displayed no effect on progesterone-induced hyperactivation, indicating that ABHD2 activity is not required for this process. At the mechanistic level, ABHD2 inhibitors did not affect intracellular Ca^{2+} levels nor progesterone-induced Ca^{2+} influx in human sperm. Notably, we also did not observe any impact of MAFP and lupeol on sperm hyperactivation. Only pristimerin completely inhibited the enzymatic activity of truncated ABHD2, while it had no effect on the full-length protein. This implies that hyperactivation may still be regulated by a mechanism that involves hydrolysis of 2-AG which can be prevented by pristimerin but is independent of ABHD2.

In summary, our data do not support the role of ABHD2 as a non-genomic progesterone receptor. Furthermore, we did not observe an influence of steroids on the enzymatic activity nor thermal stability of purified ABHD2. Finally, the presence of sub-micromolar or covalent ABHD2 inhibitors did not affect progesterone-induced Ca^{2+} influx nor hyperactivation of human spermatozoa. Therefore, we conclude that while the molecular mechanism of the non-genomic steroid action on human sperm still remains elusive, it is not dependent on ABHD2.

Material and Methods

<u>Creation of ABHD2 protein expression vectors</u>

The gene for human ABHD2 protein (Uniprot ID P08910) was introduced through Ligation Independent Cloning with In-Fusion enzyme (Clontech) into several vectors for expression tests. After testing various expression constructs in *E. coli*, SF9 cells, and mammalian cells, we were able to obtain expression for ABHD2 amino acids 33-425, in which a predicted transmembrane domain (amino acids 1-32) is removed. This construct was expressed in the *E. coli* expression vector pET28-FLAG which was derived from pET28a(+). This vector confers kanamycin resistance and expresses an N-terminal His6-FLAG sequence under T7/Lac regulation. The resulting plasmids were propagated in *E. coli* DH5α cells, and sequence-verified. For expression, the plasmids were transformed into chemically competent BL21(DE3)-R3-pRARE2 *E. coli* cells[40] and propagated in media containing kanamycin (50 µg/mL) and chloramphenicol (34 µg/mL).

For expression in insect cells, a codon optimized insert encoding for full-length human ABHD2 was synthesized at Thermofisher Scientific and cloned via Gateway technology (Invitrogen) into pD-INS26, a vector backbone produced in-house by modification of pVL1393 to encode for a C-terminal eGFP-6xHis tag. The first virus generation was obtained upon application of

the Baculo Gold kit (BD Pharmingen). Upon infection of SF9 cells with virus, the second and third virus generations were obtained.

Plasmids

Plasmid name	ORF description	backbone	use
ABHD2A-c051	His6-Flag-ABHD2(L33-425)	pET28a	E.coli expression of active enzyme
ABHD2A-c054	His6-Flag-ABHD2(L33-425) S207A	pET28a	E.coli expression of inactive mutant
pcDNA-ABHD2-Flag	ABHD2 (Full-length) with C-terminal Flag3 tag	pcDNA3	Mammalian expression for immunofluorescence
ABHD2-HiBit	ABHD2(L33-425) with N-terminal HiBit tag (Promega)		Cellular Thermal stabilization

Full ORF sequences are provided in the supplementary materials.

Expression and Purification of Recombinant ABHD2

E. coli cells were grown in Terrific Broth with 0.8% glycerol, chloramphenicol and kanamycin, in UltraYield flasks or the LEX bioreactor system (Harbinger Biotechnology and Engineering Corp., Ontario, Canada) and each flask was inoculated with overnight culture (0.01:1 overnight culture: media). The cells were incubated at 37 °C until the OD600 reached ~ 1.0; this step generally took 3-4 h. The cultures were then cooled for 20 min by reducing the temperature to 15 °C. The expression of each protein was induced with the addition of IPTG to a final concentration of 0.3 mM. The induction was carried out for 14-18 h at 15 °C.

After overnight induction, the cells were harvested by centrifuging at 6,250 RCF for 15 minutes. Cell pellets were resuspended in Sonication Buffer (50 mM Tris pH 8, 500 mM NaCl, 10% Glycerol, 1% Triton X-100, 2 mM TCEP). We did not add any serine protease inhibitors, as these may inhibit ABHD2. Resuspended cells were sonicated for 7 minutes (total sonication time) in intervals of 8 seconds on, 30 seconds off, followed by a 10 minute incubation with Benzonase. Cell debris was removed by centrifugation at 36,000 RCF for 50 min. The clarified lysate was incubated with nickel beads (5 mL of beads per 10 L of cells), then the beads were washed with 20 CV Lysis buffer (50 mM Tris pH 8, 500 mM NaCl, 10 mM Imidazole, 10% Glycerol, 2 mM TCEP), 32 CV Wash Buffer (50 mM Tris pH 8, 1 M NaCl, 30 mM Imidazole, 2 mM TCEP) and 4 CV Lysis buffer to lower salt concentration. Samples were eluted in Elution Buffer (50 mM Tris pH 8, 500 mM NaCl, 250 mM Imidazole, 10% Glycerol, 2 mM TCEP). Purification was carried out either by gravity flow or on an AKTAxpress purification machine using HisTrap-excel columns.

Elution fractions were pooled, concentrated to 5 mL, filtered via a 0.45 µm syringe filter, and loaded on a HiLoad 16/600 Superdex 75 pg. The protein eluted as a tetramer, and pure elution fractions were concentrated in 20 mM HEPES, pH 8, 500 mM NaCl, 10 % glycerol, 1 mM TCEP, snap frozen in an ethanol/dry ice bath, and stored at -80 °C.

Expression and purification of full-length ABHD2

For protein expression, SF9 cells were infected with a multiplicity of infection of 0.1 of the third virus generation and the cell pellet was harvested 48 hours after infection by centrifugation. For cell lysis, the pellet was resuspended in solubilization buffer (50mM Tris-HCl pH 7.5 @RT, 500 mM NaCl, 10mM imidazole, 2mM EDTA, 0.5mM DTT, 1% DDM and 0.1% CHS (Anatrace), 0.1µg/mL Benzonase) and incubated for one hour at 4°C. Solubilization was facilitated by 7-10 strokes with a glass Dounce homogenizer. After centrifugation at 35.000 g for 1h at 4°C, the supernatant was harvested, filtered through a 125 µM nylon mesh and diluted 1.7-fold in wash buffer (50mM Tris-HCl pH 7.5 @RT, 500mM NaCl, 40mM imidazole, 1mM DTT, 0.1% DDM and 0.01% CHS). The diluted supernatant was loaded onto a His trap FF crude affinity column, washed and eluted via a continuous gradient to elution buffer (50mM Tris-HCl pH 7.5 @RT, 300 mM NaCl, 400mM imidazole, 1 mM DTT, 0.1% DDM and 0.01% CHS). The c-terminal eGFP-6xHis tag was cleaved overnight upon addition of TEV protease and incubation during dialysis into dialysis buffer (50mM Tris-HCl pH 7.5 @RT, 300 mM NaCl, 10mM imidazole, 2mM DTT, 0.1% DDM and 0.01% CHS). The protein was loaded again onto a His trap FF crude column equilibrated in wash buffer and the flow-through of the re-chromatography was collected, containing the cleaved ABHD2 protein. The protein was concentrated with a 30kDa cutoff filter (Amicon) and loaded onto a S200 10/300 column (GE Healthcare) equilibrated in SEC buffer (50mM Tris-HCl pH 7.5 @RT, 300 mM NaCl, 1mM DTT, 0.1% DDM and 0.01% CHS). Fractions of the chromatogram peak containing the ABHD2 protein were concentrated to 2mg/mL and flash-frozen in liquid nitrogen.

Purification of ABHD10 and ABHD11

Constructs encoding amino acids T53 – N306 of human ABHD10 and residues V34 – V315 of human ABHD11 were cloned in vector pNIC28-Bsa4[40], which adds a N-terminal His6 tag followed by a TEV protease cleavage site. Both proteins were expressed and purified from E. coli cells as described for ABHD2, except that Triton X100 was not included in the lysis buffer.

Enzymatic assays

Enzymatic activity of ABHD2 was investigated by a fluorometric assay using 7-hydroxycoumarinyl arachidonate (7-HCA; Sigma, Cat-No.: U0383-10MG) as substrate. Each reaction (200 µL volume in 96-well plates) contained 10 nM of recombinantly purified ABHD2 and 10 µM 7-HCA in 20 mM HEPES, pH 8, 500 mM NaCl, 10 % glycerol, 1 mM TCEP, and 2 % DMSO.

For experiments involving compounds, 40 µL of 50 nM ABHD2 were pre-incubated on ice for 30 min with 50 µM compound or DMSO in 20 mM HEPES, pH 8, 500 mM NaCl, 10 % glycerol, 1 mM TCEP; all reactions were normalized to 2 % DMSO. The plates were then transferred

to 37 °C for 5 min and the enzymatic reaction was initiated by addition of 160 µL of 37 °C pre-warmed substrate solution in identical buffer to achieve final concentrations of 10 nM ABHD2. For initial screens, compounds were added at 10 µM in duplicate, while for IC50 determination, compounds were spotted via echo-dispensing in triplicates at concentrations ranging from 0.00625, 0.00125, 0.0025, 0.0050, 0.0100, 0.0250, 0.500, 1, 5, 10, 50, and 100 µM.

The reactions were incubated for 10 minutes at 37°C and the fluorescence (λ_{ex} = 335 nm and λ_{em} = 450 nm) was monitored continuously in 30 s intervals on a SpectraMax iD3 (MolecularDevices).

To determine Michaelis-Menten kinetics, 5 nM ABHD2 were incubated as described above for 20 min with varying concentrations of 7-HCA, ranging from 0, 0.025, 0.05, 0.10, 0.25, 0.4, 0.5, 1, 2.5, 5, 7.5, and 10 µM. The amount of product produced was determined by a standard curve of known umbelliferone concentrations using linear regression.

Statistical analysis was performed using GraphPad Prism 10 for MacOS (version 10.3.1). IC50 values were determined by a four-parameter dose response curve using a variable Hill slope. Michaelis constant and v_{max} were determined by fitting the reaction rate against substrate concentrations via the Michaelis-Menten equation.

The Full-length ABHD2 was assayed in buffer containing 50 mM HEPES, pH 7.5, 150 mM NaCl, 0.01% Triton X-100, 6 nM FL-ABHD2 and RB. Reactions were incubated for 100 minutes at room temperature. The product was measured by fluorescence intensity (Ex 335 nm, Em 450 nm).

ABHD10 and ABHD11 were assayed in a colorimetric assay using p-nitrophenyl butyrate as substrate. 125 nM ABHD11 and 1500 nM ABHD10 (both in 150 mM NaCl, 20 mM HEPES, pH7.5, 2 % DMSO) were incubated in a 96-well plate for 30 min at 4 °C in the presence of 50 µM compound. Afterwards the plate was incubated for 2 min at 37 °C before addition of 160 µl substrate solution (150 mM NaCl, 20 mM HEPES, pH7.5, 2 % DMSO, 625 µM p-nitrophenyl butyrate), pre-warmed 37 °C, to a total reaction volume of 200 µl. Final assay concentrations were 25 nM ABHD11, 300 nM ABHD10, and 500 µM p-nitrophenyl butyrate. The substrate was mixed to the substrate solution just before adding to the enzyme solutions. Absorbance was monitored at 405 nm for 20 min continuously in 30 s intervals on a SpectraMax iD3 (MolecularDevices).

Compound synthesis

All chemical reagents were purchased from Sigma-Aldrich, Merck, Fisher Scientific, Apollo Scientific, or Fluorochem and used without further purification. Solvents were evaporated under reduced pressure using a Büchi rotary evaporator. Room temperature is defined as between 18–22 °C. Thin-layer chromatography (TLC) was performed on Merck Silica Gel 60

F 254 precoated aluminium plates (0.2 mm) visualized with UV irradiation (254 nm) and stained with aqueous basic potassium permanganate solution. Reverse phase flash column chromatography was carried out using Biotage® Sfär C18 columns and the Biotage® Selekt flash purification system. ^{1}H and ^{13}C NMR spectra were recorded using Bruker Avance III 400. Chemical shifts (δ) are quoted in parts per million (ppm) and are referenced to the residual solvent peak: $CDCl_3$ (δ 7.26 ppm in ^{1}H and δ 77.2 ppm in ^{13}C). Coupling constants (*J*) are quoted in Hertz (Hz). The ^{1}H NMR spectra are reported as follows: ppm (multiplicity, coupling constants, number of protons, assignment). NMR assignments use numbering independent from IUPAC, using two-dimensional (COSY, HSQC, HMBC) NMR spectroscopy to assist the assignment. Analytical liquid chromatography mass spectrometry (LCMS) was performed on an Agilent Infinity 1260 II system consisting of a quaternary pump (G7111A) and a diode array detector WR (G7115A) coupled to an InfinityLab LC/ MSD (G6125B) using ESI. An Agilent Poroshell 120 EC-C18 column (2.7 µm, 4.6 mm × 50 mm) was used at a flow rate of 1.5 mL/min with a mobile phase of 0.05% formic acid in H_2O and 0.05% formic acid in MeCN. High-resolution mass spectrometry (HRMS) was performed on an Agilent 6545XT AdvanceBio LC/Q-TOF using ESI in positive detection. Chiral high-performance liquid chromatography (HPLC) was performed on an Agilent Infinity 1200 system consisting of a quaternary pump (G1311A) and a diode array detector (G1315D) using a Chiralcel OD-H column.

Differential scanning fluorimetry

4 µM ABHD2 were incubated with 40 µM compound for 30 min on ice in 20 mM HEPES, pH 8, 500 mM NaCl, 10 % glycerol, 1 mM TCEP, and 2 % or 4% DMSO, in presence of compounds or steroids, respectively. Samples were spun at 15000x*g* before transfer into Prometheus™ NT.48 Capillaries. After thermal equilibration at 25 °C for 5 min, samples were heated to 95 °C with a linear ramp of 1 °C/min on a Prometheus NT.48 instrument (NanoTemper Technologies). Changes in fluorescence emission at 330 and 350 nm were recorded in triplicates.

Melting temperature of proteins was determined as inflection points of a sigmoidal fit of ratio of 350 nm/330 nm with temperature dependence.

Cell Immunofluorescence

U2OS cells plated on glass coverslips were transfected with 1 µg of C-terminally tagged, full-length ABHD2-FLAG using X-tremeGENE™ HP DNA Transfection Reagent (Sigma), following the manufacturer's instructions. Four hours later, the media was replaced with DMEM (supplemented with 10% FBS, penicillin (100 U/mL) and streptomycin (100 µg/mL). All

subsequent treatments were in phosphate-buffered saline (PBS) containing the indicated additives. The next day, cells were fixed with 2% methanol-free PFA for 10 min, either permeabilized or not with 0.1% Triton X-100 for 10 min, and blocked with 2% BSA for 30 min. The cells were then incubated with mouse anti-flag (Sigma, F1804) at 4°C overnight, followed by incubation with Alexa Fluor 488-conjugated goat anti-mouse IgG (Cell Signaling Technology, 4408) at room temperature for 1 h. Coverslips were mounted using Fluoroshield™ with DAPI (Sigma, F6057) and image acquisition was performed using the Quorom Spinning Disk Confocal system, based on a Leica DMi8 microscope.

Cellular thermal shift assay

HEK293T cells were plated in 6-well plates (1e6/well) and reversely transfected with 0.2 µg of N-terminally HiBIT –tagged ABDH2 and 1.8 µg of empty plasmid using X-tremeGene XP transfection reagent, following manufacturer's instructions. Next day cells were trypsinized and resuspended in OptiMEM (no phenol red) at density 2e5/mL.After the addition of compounds or DMSO (the same DMSO concentration in all samples), the cells were transferred to 96-well PCR plates (40 µL/well), incubated for 1 h at 37 °C and heated at temperatures ranging from 37°C to 60°C in a thermocycler for 3 min. After a further 3 min at RT, 40 µL of LgBIT solution (200 nM LgBIT, 2% NP-40, and protease inhibitors in OptiMEM (no phenol red) was added and incubated at RT for 10 min. Next, 20 µL of NanoGlo substrate (8 µL/mL, Promega) was added, mixed gently and 20 µL was transferred to 384 white plates in triplicates and bioluminescence signal was read in ClarioStar plate reader. The results and MEAN+/- SD. Recovery of soluble protein after heating was assessed by luminescence detection of reconstituted luciferase; the signal was normalized to non-heated controls kept at 37 °C.

For examining multiple compounds, a single heating temperature of 50°C was selected, and normalized to cells incubated at 37°C

Sperm hyperactivation assay

Human sperm samples were purchased from the European Sperm Bank (ESB; https://www.europeanspermbank.com/en), that complies with all applicable laws, regulations and practices and all other governmental and regulatory standards, specifications, and guidelines applying to human sample donations. Donors were healthy and normozoospermic (according to the World Health Organization criteria; WHO, 2021) and signed informed consent forms. Semen samples were processed by density gradient centrifugation and washing before cryopreservation.

Cryopreserved sperm samples (n = 6) were thawed by a 5 min incubation at room temperature and washed twice using capacitating SpermActive medium (Gynemed; Sierksdorf, Germany).

Samples were diluted to a concentration of 6-10 x 10^6 sperm/mL using SpermActive and incubated at 37 °C, 5 % CO_2. After 1 h, 2 h and 3 h incubation, aliquoted sperm suspensions were treated with DMSO or with 10 µM of compound 1, compound 3, MAFP, lupeol and pristimerin (each inhibitor individually; all were dissolved in DMSO) for 1 h at 37 °C, 5 % CO_2. Progesterone (P4; 1 µM) or DMSO was added 5 min before motility analysis.

Sperm motility was analyzed by the CASA system CEROSII™ Animal Motility (software version 1.16; Hamilton Thorne, Beverly, MA, USA), using a Axiolab 5 microscope (Zeiss, Germany) equipped with a TPi-SX Thermal Plate (Tokai Hit; Shizuoka-ken, Japan) and a JAI CM-040-GE CCD camera (JAI; Tokio, Japan). Pre-warmed Leja slides (20 µm depth; Leja Products B.V., Nieuw Vennep, The Neatherlands) were used and the capillary correction was set to 1.3. Slides were cleaned with lens-cleaning paper and each chamber was filled with 6 µL sperm suspensions, by capillary action. Sperm tracks were captured at 37°C with a 10x negative phase objective, by recording 60 frames at a 60 Hz frame capture speed. The camera was set to 4 ms exposure, with 600 gain. For each sample/condition analyzed, 300-500 motile sperm were recorded, from at least 10 non-overlapping fields. Hyperactive sperm was detected using the SORT function and the following Bollean argument: VCL > 150 µm/s and LIN < 50 % and ALH > 7 µm. The % of hyperactive sperm was normalized to the % of motile sperm.

For each sample, 21 measurements were performed: 7 conditions after 3 different capacitation times. Since the capacitation time did not affect the outcomes, for each condition (within each sample), the 3 measurements were considered technical replicates, and the mean values were calculated. Results were expressed as % relative to controls (DMSO).
Statistical analysis was performed using GraphPad Prism 10 for Windows (version 10.2.3). Data normality was assessed using Kolmogorov-Smirnov test. Comparisons of the different conditions with control (DMSO) and with P4 were done using repeated measures one-way ANOVA and Holm-Šídák´s multiple comparisons test. *P* values < 0.05 were considered significant.

<u>Calcium influx in sperm:</u>
Semen samples were obtained from normozoospemic (according to WHO) healthy volunteers with prior written consent, under approval from the ethical committees of the medical association Westfalen-Lippe and the medical faculty of the University of Münster (4INie, 2021-402-f-S). Semen samples were produced by masturbation and ejaculated into plastic containers. The samples were allowed to liquefy for 15–60 min at 37 °C, and motile sperm were purified by swim-up procedure: liquefied semen (0.5–1 mL) was directly layered in a 50-

mL falcon tube below 4 mL of human tubular fluid (HTF) medium containing 97.8 mM NaCl, 4.69 mM KCl, 0.2 mM $MgSO_4$, 0.37 mM KH_2PO_4, 2.04 mM $CaCl_2$, 0.33 mM Na-pyruvate, 21.4 mM lactic acid, 4 mM $NaHCO_3$, 2.78 mM glucose, and 21 mM HEPES (pH 7.35 was adjusted with NaOH). Motile sperm were allowed to swim up into HTF for 60–90 min at 37 °C. Sperm were washed two times (700 × g, 20 min, 37 °C) and resuspended in HTF containing 3 mg/mL HSA at a density of 1×10^7 sperm/mL. Changes of $[Ca^{2+}]_i$ in motile human sperm were measured essentially as in (PMID 29723408), using a plate reader (Fluostar Omega, BMG Labtech) with 384-well plates and a fluorescence-based readout. Sperm, purified by the swim-up procedure, were loaded with Fluo4-AM (5 µM, ThermoFisher) and Pluronic F-127 (0.05% w/v) for 20 min. Centrifugation at 700 × g for 5 min, removal of the supernatant and resuspension to 5×10^6 sperm/mL in HTF medium removed excess dye. For the experiments, wells were filled with 50 µL of the dye-loaded sperm suspension. Fluorescence was excited at 480 nm, and emission was recorded at 520 nm. After recording a baseline for at least 60 seconds, 25 µL of test compound solutions were added and fluorescence response recorded. After 4 min, 7.5 µL of progesterone (final concentration 3 µM) was added and ensuing changes in fluorescence were recorded. For examination of compound-evoked Ca^{2+} signal, basal fluorescence (F) was determined before addition of compounds. For determination of inhibitory effects of compounds on progesterone-evoked Ca^{2+} signals, basal fluorescence (F) was determined before addition of progesterone. Data from fluorescence recordings were analyzed in GraphPad Prism version 9.4.0. Each compound was tested as duplicate ($n \geq 3$) with sperm from at least two different donors on at least two different days.

Acknowledgements

This project is funded by the Bill and Melinda Gates Foundation.

The authors are also grateful to the Structural Genomics Consortium (SGC), a registered charity (No. 1097737) that received funds from Bayer AG, Boehringer Ingelheim, Bristol Myers Squibb, Genentech, Genome Canada through Ontario Genomics Institute, Janssen, Merck KGaA, Pfizer, and Takeda. This project received funding from the Innovative Medicines Initiative 2 Joint Undertaking (JU) under Grant Agreement No. 875510. The JU receives support from the European Union's Horizon 2020 research and innovation programme, EFPIA, Ontario Institute for Cancer Research, Royal Institution for the Advancement of Learning, McGill University, Kungliga Tekniska Hoegskolan, and Diamond Light Source Limited. This communication reflects the views of the authors and neither IMI nor the European Union, EFPIA or any Associated Partners are liable for any use that may be made of the information contained herein.

LT, CB, and TS were supported by the Deutsche Forschungsgemeinschaft (DFG, German Research Foundation) - project numbers 329621271 (CRU326; CB, TS), and 404595355 (Research Training Group “Chemical biology of ion channels (Chembion)'; LT, TS).
We thank Jeff Mowat (Johnson and Johnson, Antwerp) for advice in his role as Pharma Champion for the open science project associated with this research (https://github.com/StructuralGenomicsConsortium/CNP6-ABHD2), where anyone is free to contribute.

References

1. United Nations Department of Economic and Social Affairs Population Division. *World Family Planning 2022: Meeting the changing needs for family planning: Contraceptive use by age and method*. (2022).
2. Cheung, E. & Free, C. Factors influencing young women’s decision making regarding hormonal contraceptives: A qualitative study. *Contraception* **71**, 426–431 (2005).
3. Howard, S. A. & Benhabbour, S. R. Non-Hormonal Contraception. *J. Clin. Med.* **12**, (2023).
4. Kaneshiro, B. & Aeby, T. Long-term safety, efficacy, and patient acceptability of the intrauterine Copper T-380A contraceptive device. *Int. J. Womens. Health* **2**, 211–220 (2010).
5. Akintomide, H., Brima, N., Mansour, D. J. & Shawe, J. Copper IUD continuation, unwanted effects and cost consequences at 1 year in users aged under 30–a secondary analysis of the EURAS-IUD study. *Eur. J. Contracept. Reprod. Heal. Care* **26**, 175–183 (2021).
6. Phillips, S. J. *et al.* Continuation of copper and levonorgestrel intrauterine devices: a retrospective cohort study. *Am. J. Obstet. Gynecol.* **217**, 57.e1-57.e6 (2017).
7. Akintomide, H., Barnes, P., Brima, N. & Mansour, D. Higher discontinuation rate with a standard-sized compared to a small-sized ‘gold standard’ copper intrauterine device: A case-control review. *BMJ Sex. Reprod. Heal.* **45**, 263–268 (2019).
8. Bellizzi, S., Mannava, P., Nagai, M. & Sobel, H. L. Reasons for discontinuation of contraception among women with a current unintended pregnancy in 36 low and middle-income countries. *Contraception* **101**, 26–33 (2020).
9. Ren, D. *et al.* A sperm ion channel required for sperm motility and male fertility. *Nature* **413**, 603–609 (2001).
10. Trebichalská, Z. & Holubcová, Z. Perfect date—the review of current research into molecular bases of mammalian fertilization. *Journal of Assisted Reproduction and Genetics* vol. 37 243–256 (2020).
11. Kirichok, Y., Navarro, B. & Clapham, D. E. Whole-cell patch-clamp measurements of

spermatozoa reveal an alkaline-activated Ca2+ channel. *Nature* **439**, 737–740 (2006).

12. Lishko, P. V., Botchkina, I. L. & Kirichok, Y. Progesterone activates the principal Ca2+ channel of human sperm. *Nature* **471**, 387–392 (2011).
13. Strünker, T. *et al.* The CatSper channel mediates progesterone-induced Ca2+ influx in human sperm. *Nature* **471**, 382–387 (2011).
14. Miller, M. R. *et al.* Unconventional endocannabinoid signaling governs sperm activation via the sex hormone progesterone. *Science (80-.).* **352**, 555–559 (2016).
15. Suarez, S. S. Formation of a reservoir of sperm in the oviduct. *Reprod. Domest. Anim.* **37**, 140–143 (2002).
16. Wang, S. & Larina, I. V. In vivo three-dimensional tracking of sperm behaviors in the mouse oviduct. *Dev.* **145**, (2018).
17. Young, S. *et al.* Human fertilization in vivo and in vitro requires the CatSper channel to initiate sperm hyperactivation. *J. Clin. Invest.* **134**, (2024).
18. Williams, H. L. *et al.* Specific loss of CatSper function is sufficient to compromise fertilizing capacity of human spermatozoa. *Hum. Reprod.* **30**, 2737–2746 (2015).
19. Luo, T. *et al.* A novel copy number variation in CATSPER2 causes idiopathic male infertility with normal semen parameters. *Hum. Reprod.* **34**, 414–423 (2019).
20. Patrat, C., Serres, C. & Jouannet, P. The acrosome reaction in human spermatozoa. *Biol. Cell* **92**, 255–266 (2000).
21. Ikawa, M., Inoue, N., Benham, A. M. & Okabe, M. Fertilization: A sperm's journey to and interaction with the oocyte. *J. Clin. Invest.* **120**, 984–994 (2010).
22. Bianchi, E. & Wright, G. J. Sperm Meets Egg: The Genetics of Mammalian Fertilization. *Annu. Rev. Genet.* **50**, 93–111 (2016).
23. Lord, C. C., Thomas, G. & Brown, J. M. Mammalian alpha beta hydrolase domain (ABHD) proteins: Lipid metabolizing enzymes at the interface of cell signaling and energy metabolism. *Biochimica et Biophysica Acta - Molecular and Cell Biology of Lipids* vol. 1831 792–802 (2013).
24. Mannowetz, N., Miller, M. R. & Lishko, P. V. Regulation of the sperm calcium channel CatSper by endogenous steroids and plant triterpenoids. *Proc. Natl. Acad. Sci. U. S. A.* **114**, 5743–5748 (2017).
25. De Toni, L. *et al.* Membrane Cholesterol Inhibits Progesterone-Mediated Sperm Function through the Possible Involvement of ABHD2. *Int. J. Mol. Sci.* **24**, (2023).
26. Brenker, C. *et al.* Action of steroids and plant triterpenoids on CatSper Ca2+ channels in human sperm. *Proc. Natl. Acad. Sci. U. S. A.* **115**, E344–E346 (2018).
27. Jiang, F. *et al.* Progesterone activates the cyclic AMP-protein kinase A signalling pathway by upregulating ABHD2 in fertile men. *J. Int. Med. Res.* **49**, 300060521999527 (2021).

28. Agarwal, A. *et al.* Male infertility. *Lancet* **397**, 319–333 (2021).
29. Baggelaar, M. P. *et al.* ABHD2 Inhibitor Identified by Activity-Based Protein Profiling Reduces Acrosome Reaction. *ACS Chem. Biol.* **14**, 2295–2304 (2019).
30. Clemente, J. C. *et al.* Screening and characterization of human monoglyceride lipase active site inhibitors using orthogonal binding and functional assays. *J. Biomol. Screen.* **17**, 629–640 (2012).
31. Miceli, M. *et al.* Set-up and validation of a high throughput screening method for human monoacylglycerol lipase (MAGL) based on a new red fluorescent probe. *Molecules* **24**, (2019).
32. Iglesias, J. *et al.* Simplified assays of lipolysis enzymes for drug discovery and specificity assessment of known inhibitors. *J. Lipid Res.* **57**, 131–141 (2016).
33. Wang, Y., Chanda, P., Jones, P. G. & Kennedy, J. D. A Fluorescence-Based Assay for Monoacylglycerol Lipase Compatible with Inhibitor Screening. *Assay Drug Dev. Technol.* **6**, 387–393 (2008).
34. Jumper, J. *et al.* Highly accurate protein structure prediction with AlphaFold. *Nature* **596**, 583–589 (2021).
35. Hsu, K. L. *et al.* DAGLβ inhibition perturbs a lipid network involved in macrophage inflammatory responses. *Nat. Chem. Biol.* **8**, 999–1007 (2012).
36. Adibekian, A. *et al.* Click-generated triazole ureas as ultrapotent in vivo-active serine hydrolase inhibitors. *Nat. Chem. Biol.* **7**, 469–478 (2011).
37. Rehfeld, A. Revisiting the action of steroids and triterpenoids on the human sperm Ca2+ channel CatSper. *Mol. Hum. Reprod.* **26**, 816–824 (2020).
38. Blackmore, P. F., Beebe, S. J., Danforth, D. R. & Alexander, N. Progesterone and 17α-hydroxyprogesterone. Novel stimulators of calcium influx in human sperm. *J. Biol. Chem.* **265**, 1376–1380 (1990).
39. Schierling, T. *et al.* Synthesis and Functional Characterization of Novel RU1968-Derived CatSper Inhibitors with Reduced Stereochemical Complexity. *ACS Pharmacol. Transl. Sci.* **6**, 115–127 (2023).
40. Savitsky, P. *et al.* High-throughput production of human proteins for crystallization: The SGC experience. *J. Struct. Biol.* **172**, 3–13 (2010).

Figures

Figure 1. Characterisation of ABHD2 inhibitors. (A) structures of the inhibitors with enzymatic IC50 values and T_M shifts obtained with ABHD2(L33-E425). (B) representative inhibition curves. (C) representative melting and derivative curves

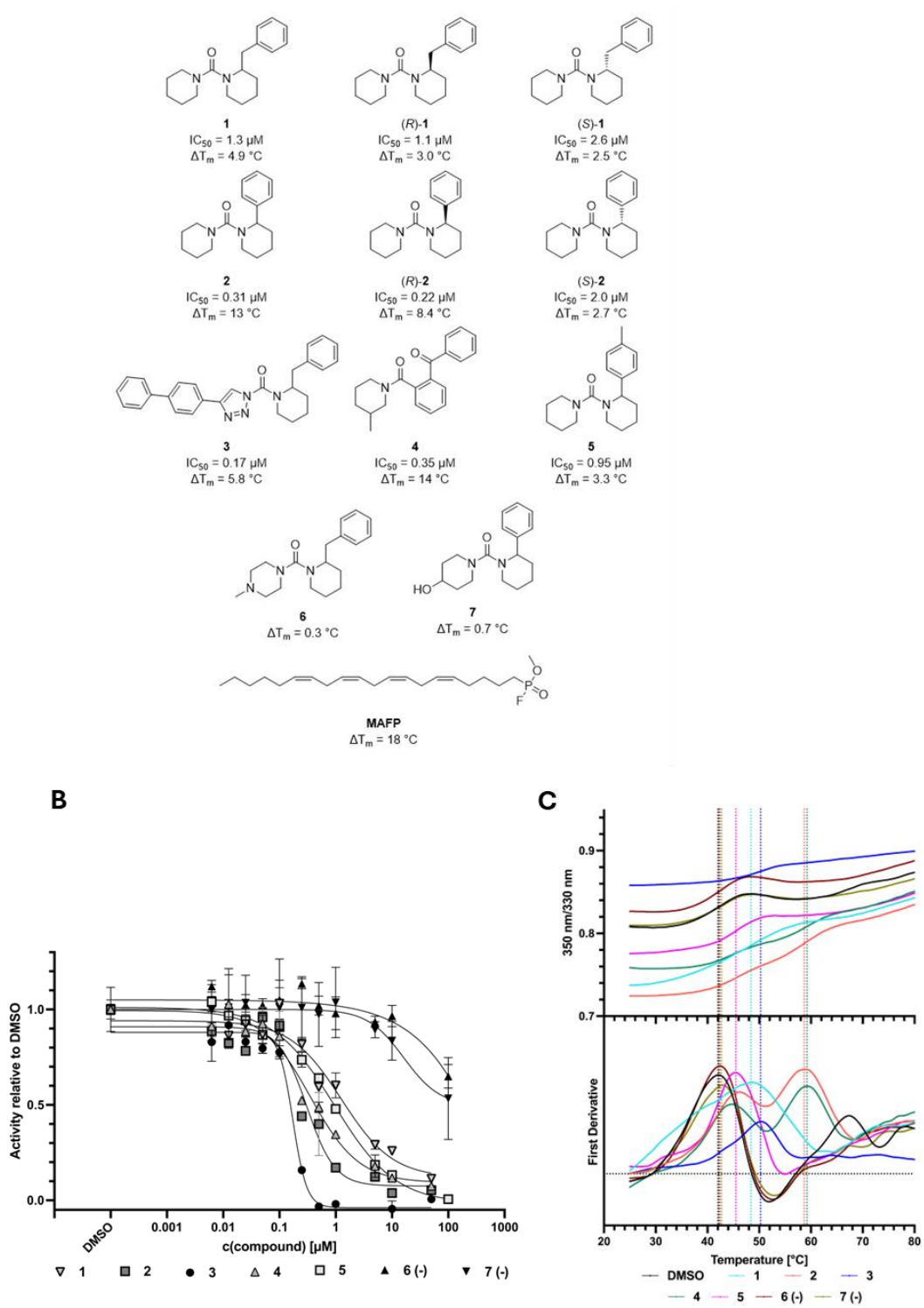

Figure 2: Endogenous steroids (5 µM) do not modulate the enzymatic activity (A) nor lead to thermal stabilization (B) of ABHD2(L22-E425).

A. Enzymatic activity.
B. DSF curves of representative compounds

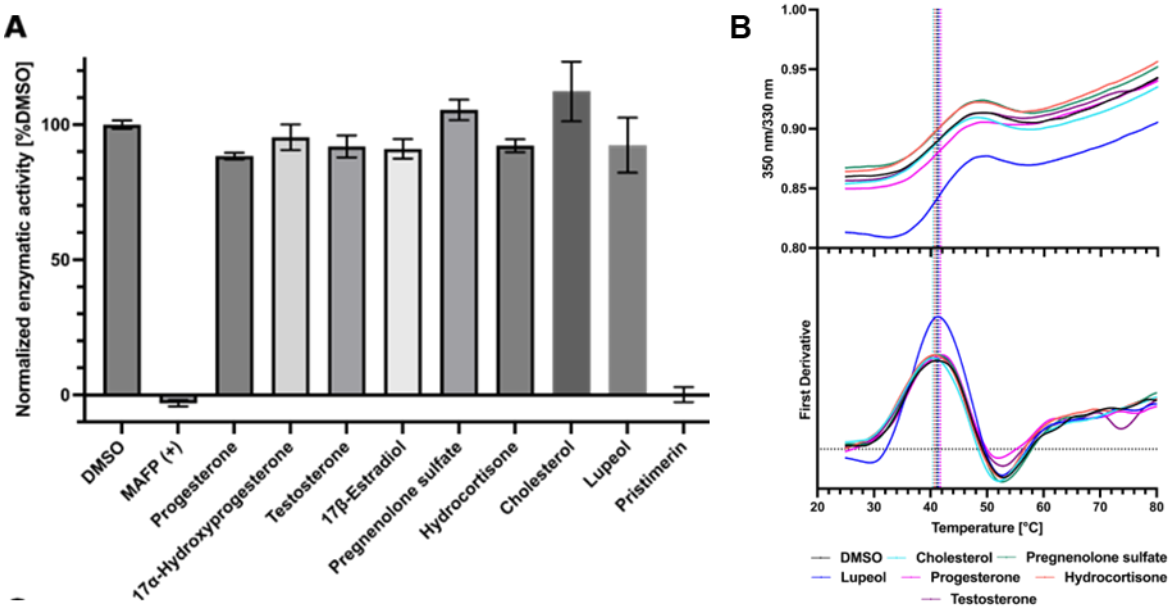

Figure 3: Thermostabilization of ABHD2 by inhibitors in intact cells. A. Cells were incubated with compound 1, compound 6 (171) or DMSO followed by a 3 minute incubation at the indicated temperatures. Remaining ABHD2 protein levels were monitored by lumincescence and normalized to cells incubated at 37°C. B. Cells incubated with the indicated compounds, then heated for 3 minutes at 50°C. The remaining ABHD2 was measured and normalized as in A.

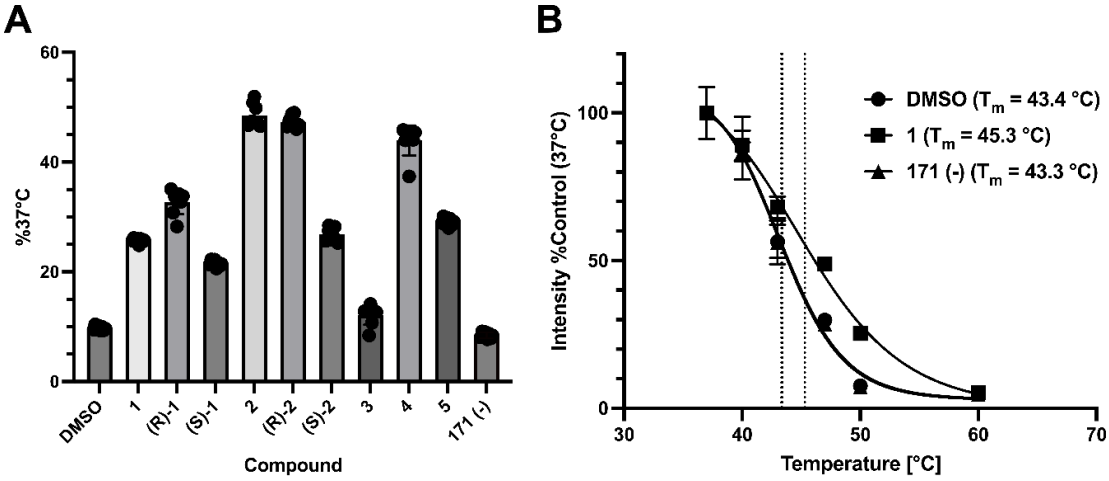

Figure 4. ABHD2 inhibitors have no impact on Progesterone (P4)-induced human sperm hyperactivation. The effect of different compounds on human sperm hyperactivation was monitored. Results (n=6) are expressed as % relative to controls (DMSO) in scatter dot plots (lines indicate means ± SEMs). **a** and **b** indicate statistically significant differences between groups ($P < 0.05$).

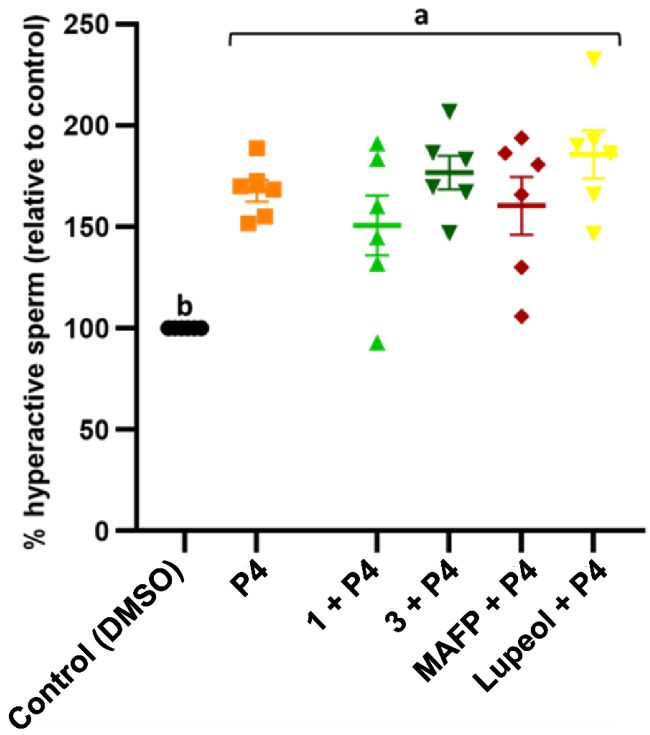

Figure 5. Action of compounds 3, *(R)*-2,and 6, as well as the CatSper inhibitor TS150, on the intracellular Ca^{2+} concentration and CatSper-mediated Ca^{2+} signals in human sperm. A, B, C, D. Representative Ca^{2+} signals in human sperm loaded with a fluorescent Ca^{2+} indicator evoked by the application of buffer (0 µM) or compound 3 (5 µM), (*R*)-2 (10 µM), 6 (10 µM), or TS150 (60 µM) and subsequent stimulation by progesterone (3 µM). ΔF/F (%) indicates the percentage change in fluorescence (ΔF) with respect to the mean basal fluorescence (F) before application of the respective compound 3, (*R*)-2, 6 and TS150, respectively. E. Mean (± SD) maximal signal amplitude evoked by progesterone (3 µM) in sperm pre-incubated with compound 3, (*R*)-2, 6, or TS150, relative to that evoked in the absence of any compound (0 µM; set to 1).

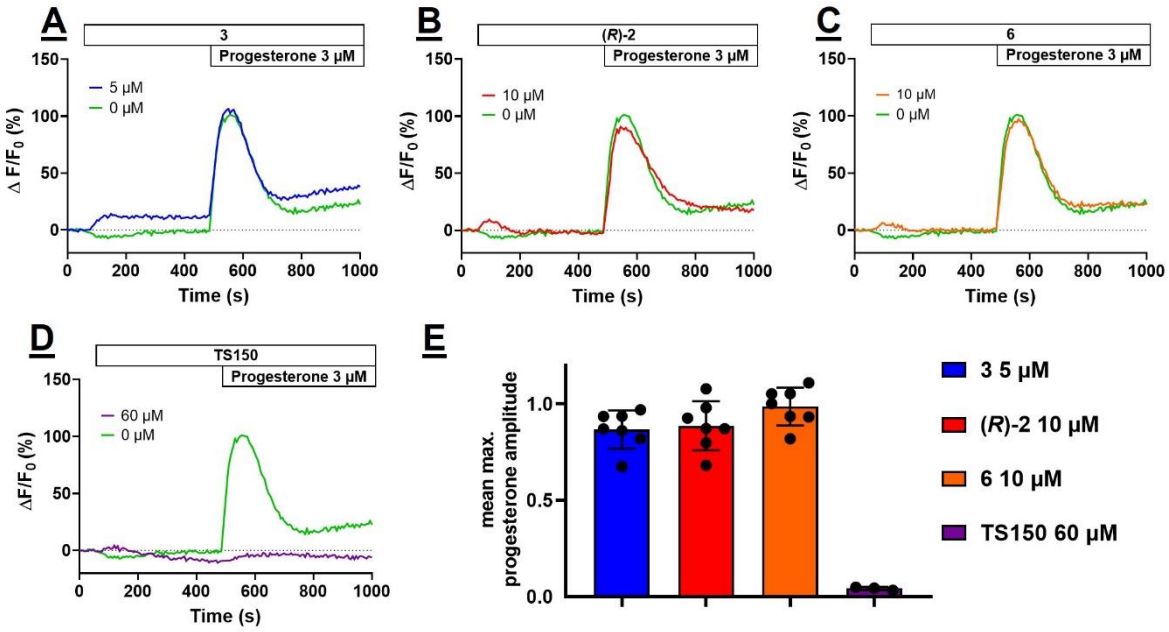

1